JOURNAL OF
BUILDING PHYSICS

Article

Journal of Building Physics
0(0) 1–27

DOI: 10.1177/1744259113480132
jen.sagepub.com
SAGE

The effect of nearby obstacles in surface condensations on external thermal insulation composite systems: Experimental and numerical study

Eva Barreira and Vasco P de Freitas

Abstract

External thermal insulation composite systems are, nowadays, quite common in European buildings, used both in new constructions and refurbishment. Unfortunately, external thermal insulation composite systems can have serious problems of biological growth causing the cladding defacement. Studies carried out in recent years allowed understanding the hygrothermal behaviour of external thermal insulation composite systems. It is known that biological growth is due to high values of surface moisture content, which depends mostly on exterior surface condensation. Despite this existing knowledge, there is little information available about the influence of obstacles near the façade on condensation and surface moisture content. In this article, the results of a field test campaign to assess the influence of obstacles on surface condensation are presented. They show that nearby obstacles influence exterior surface temperature during the night and, consequently, surface condensation. Different obstacle configurations have different effects, which may lead to stained patterns on the façade due to differential biological growth rates. The effect of nearby obstacles on exterior surface condensation, revealed during the test campaign, addressed the development of a numerical routine to simulate their influence. This routine can be used with any existing

University of Porto – Faculty of Engineering, Civil Engineering Department, Laboratory of Building Physics, Porto, Portugal

Corresponding author:
Eva Barreira, University of Porto – Faculty of Engineering, Civil Engineering Department, Laboratory of Building Physics, Rua Dr. Roberto Frias, 4200-465 Porto, Portugal.
Email: barreira@fe.up.pt

hygrothermal model with the ability to simulate explicitly the radiative balance on the exterior surface. It calculates the increase in long-wave radiation due to the obstacle as a function of its geometry and emissivity of its surface. This extra amount of radiation is added to the atmospheric radiation that is an input of the hygrothermal models. The validation of this routine was performed by comparing simulated and experimental results. An example of the practical use of this routine is also presented in this article, with the calculation of the exterior surface condensation on different façades covered with external thermal insulation composite systems, with and without nearby obstacles, and its comparison with the coating defacement that they actually present.

Keywords
External thermal insulation composite systems, hygrothermal behaviour, external surface condensations, nearby obstacles, experimental study, numerical simulation

Introduction

External thermal insulation composite systems (ETICS) have been commonly used in Portugal since the 1990 (Freitas, 2002). Despite its advantages, ETICS have revealed a serious problem of cladding defacement due to biological growth (Figure 1).

Previous studies pointed high values of surface moisture content as the cause of biological growth. External surface moisture results from the combined effect of four parameters: surface condensation, wind-driven rain, drying process and properties of the exterior layer (Barberousse et al., 2007; Becker, 2003; Blaich, 1999; Hens and Carmeliet, 2002; Krus et al., 2006; Kunzel and Sedlbauer, 2001; Sedlbauer and Krus, 2002; Venzmer et al., 2008). Although several factors

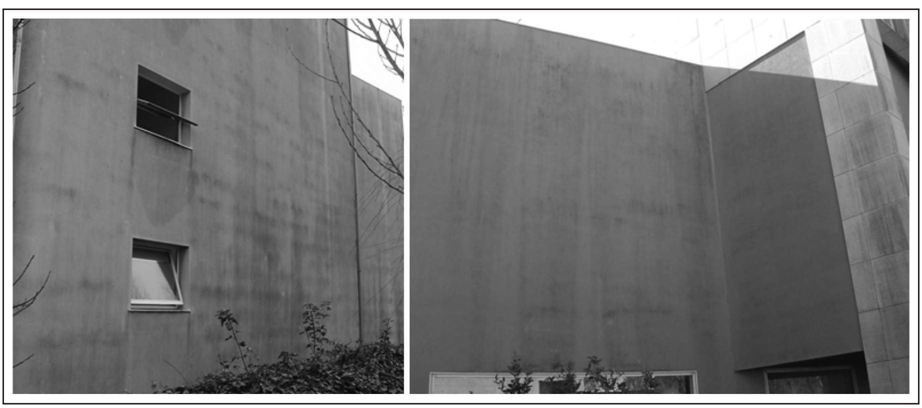

Figure 1. ETICS defacement due to biological growth (buildings in Porto, Portugal).
ETICS: external thermal insulation composite systems.

contribute to the phenomenon, surface condensation is a specific hazard for ETICS, due to the low thermal capacity of its external rendering, and has considerable impact on the phenomenon, as it occurs during all the year at equivalent intensity (Barreira and Freitas, 2013).

It is known that the long-wave radiation exchange between the exterior surface and the atmosphere, during the night, causes the ETICS surface temperature to drop (Holm et al., 2004; Zillig et al., 2003). Condensation forms when the exterior surface temperature is lower than the dew point temperature. If the drying process is not sufficiently fast, the surface moisture content remains high for long periods and increases the risk of biological growth (Krus et al., 2006).

Knowledge of the physical phenomenon made it possible to develop numerical models simulating ETICS performance, considering different conditions of use (Barreira et al., 2012; Kunzel et al., 2002). However, there is almost no information available about the influence of nearby obstacles on external condensation and surface moisture content.

Field observation of façades covered with ETICS points that whenever there is a nearby obstacle, the biological growth is less intense, even on façades facing north or west. The reliability of this empirical observation, commonly referred by producers and appliers of the system, has never been properly assessed despite its aesthetical effects.

For this reason, a field test campaign was carried out by the Building Physics Laboratory (LFC) of Porto University. The west façade of a building covered with ETICS, located in Porto University campus, was monitored simultaneously with and without different nearby obstacles. Continuous measurements of exterior climate and surface parameters were obtained. The climate parameters under study were temperature, relative humidity and atmospheric radiation. The measurements on the surface included temperature and long-wave radiation.

The results of the test campaign showed that the effect of nearby obstacles on exterior surface condensation is considerable, which addressed the development of a numerical routine to simulate their influence. The validation of this routine was performed by comparing simulated and experimental results.

Long-wave radiation exchange

Surface condensation, which occurs mostly during the night, is caused by long-wave radiation exchange between the exterior surface and the atmosphere. Although radiant exchange occurs on all exterior surfaces, it is more severe on ETICS, due to the thicker thermal insulation – which reduces the heat flow from indoor – and the thin rendering that has a very low thermal capacity (Kunzel and Sedlbauer, 2001).

The radiant balance of a building façade is affected by the building's radiation, the sky's radiation and terrestrial surface's radiation. A building, being a grey body, emits long-wave radiation that can be calculated using the Stefan–Boltzmann law (Hagentoft, 2001).

$$I_b = \varepsilon_b \cdot \sigma \cdot T_b^4 \tag{1}$$

where I_b is the radiation (W/m^2) emitted by the building, ε_b is the surface emissivity, T_b is the surface temperature (K) and σ is the Stefan–Boltzmann constant.

However, the façade absorbs part of the long-wave radiation emitted by the surrounding surfaces (terrestrial radiation) and by the sky (atmospheric radiation) (Holm et al., 2004). Terrestrial radiation is the sum of long-wave radiation emitted by the terrestrial surfaces (ground, other building façades, obstacles, etc.) that also behave as grey bodies and whose temperature is similar to the building's temperature. Therefore, terrestrial surfaces and the building emit long-wave radiation at identical intensities. Atmosphere may behave in two distinct manners. If the sky is cloudy, the atmosphere behaves like a grey body whose temperature is identical to the building's temperature and emits radiation in a continuous spectrum at intensity similar to that of terrestrial surfaces. If the sky is clear, the atmosphere stops emitting continuously for all wavelengths, and the atmosphere's emitted radiation decreases considerably. The radiation emitted by the surface is, therefore, greater than the one that reaches the surface, causing a loss of heat by radiation.

This negative balance that is not compensated by solar radiation during the night causes the building's surface temperature to decrease, which is maintained until heat transport by convection and by conduction compensates for the loss by radiation (Holm et al., 2004). Condensation takes place whenever the surface temperature is lower than the dew point temperature. The accumulation of condensed water creates conditions for biological growth.

Experimental study – assessing the influence of nearby obstacles

Setting up the test

To evaluate the influence of nearby obstacles, measurements were carried on the west façade covered with ETICS of a building located in the University of Porto campus. Two different obstacle configurations were used: vertical obstacles (*VOs*), parallel to the façade, and horizontal obstacles (*HOs*), used as a shade (Figure 2). The *VO* was placed at two different distances from the west façade (1 and 2 m), and the *HO* was made of two different materials (plastic and metallic). The parameters measured at the surface were temperature, using T-type thermocouples (copper constantan), and long-wave radiation reaching the façade, using pyrgeometers. All the devices were coupled to a data acquisition system, collecting data every 10 min. These parameters were simultaneously assessed on the façade protected by the obstacle and on the bare façade (Figure 2). The tests were carried out during three different periods of time given in Table 1. At the same time, climate

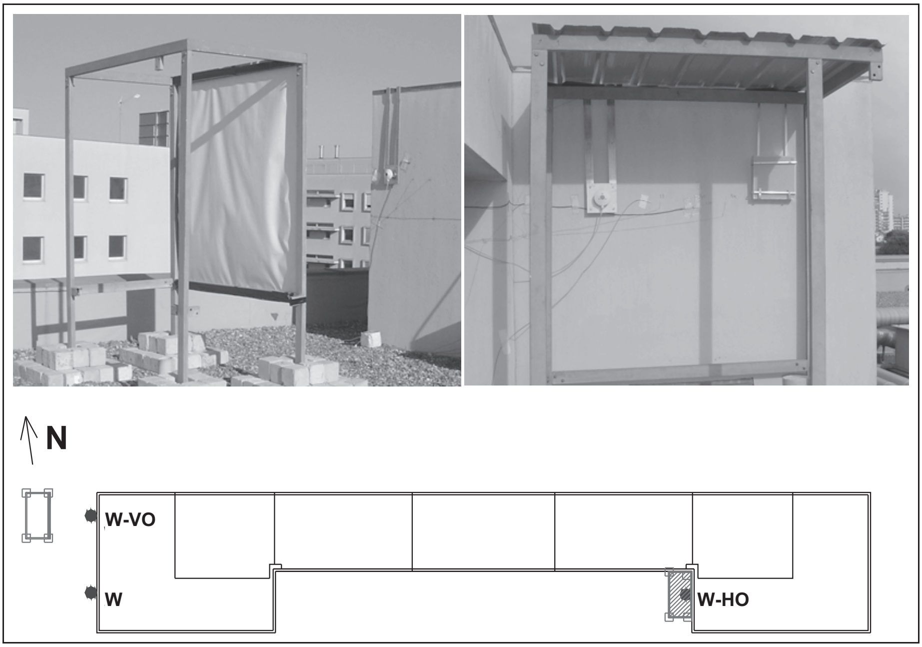

Figure 2. Vertical obstacle (*VO*), horizontal obstacle (*HO*) and layout showing the obstacles and locations of devices.

Table 1. Field test campaign description.

Reference	Obstacle	Period of time
W	None	All the time
W-VO1	Vertical obstacle	26 to 31 May 2009
	Material: plastic	04 to 09 August 2009
	Distance = 1 m	06 to 11 December 2009
W-VO2	Vertical obstacle	12 to 17 June 2009
	Material: plastic	28 July to 02 August 2009
	Distance = 2 m	17 to 22 December 2009
W-HO1	Horizontal obstacle	21 to 26 April 2009
	Material: plastic	21 to 26 July 2009
		27 October to 01 November 2009
W-HO2	Horizontal obstacle	14 to 19 April 2009
	Material: metallic	14 July to 19 July 2009
		20 October to 25 October 2009

parameters (temperature, relative humidity and atmospheric radiation) were also collected, for every 10 minutes, by the LFC weather station, located near the building under study. Information regarding the accuracy and calibration of the surface devices and about the weather station is given by Barreira (2010).

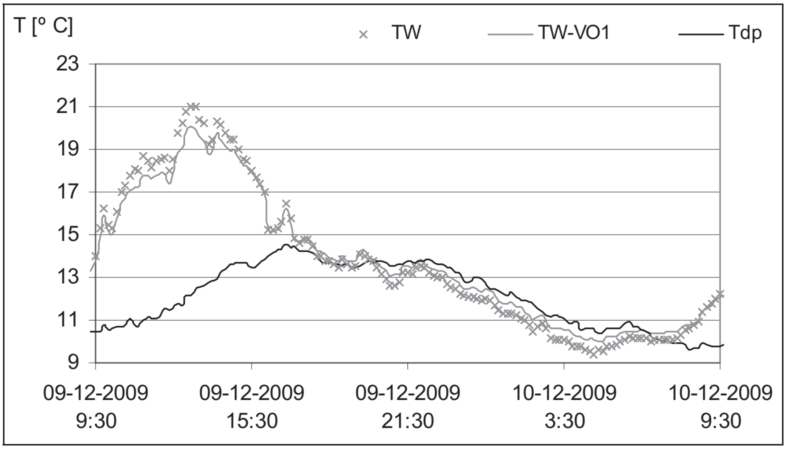

Figure 3. Temperature variation on the protected façade (*TW-VO1*) and unprotected façade (*TW*) and dew point temperature (*Tdp*), with clear sky, during one day of December 2009.

Results

VOs. The surface temperature variation on the west façade, protected by the VO at a distance of 1 m and with no nearby obstacle, is indicated in Figure 3, during one day of December 2009. This graph also indicates the dew point temperature (Tdp), which depends on the exterior temperature and relative humidity. An analysis of the measured data reveals that the unprotected façade always had lower surface temperature during the night and higher surface temperature during the day, when there was sun in the sky. This is due to the obstacle effect, which was an extra source of long-wave radiation during the night and shaded the façade when the sun was shining. When the sky was cloudy, the influence of the obstacle in the façade temperature was less intense (Figure 4).

The role of the obstacle as an extra source of long-wave radiation during the night is shown in Figure 5 that displays the long-wave radiation reaching both façades. Higher amounts of radiation always reached the protected façade, even when the sky was cloudy and both façades got similar amounts of radiation (also similar to the atmospheric radiation), as shown in Figure 6.

Equation (2) shows the radiant balance on the façade protected by the VO during the night, where its influence is obtained by an extra component of incoming radiation.

$$q = \varepsilon_b \times \left(F_{atm} \times I_{atm} + F_{ground} \times I_{ground} + F_O \times I_O\right) - I_b \tag{2}$$

where ε_b is the surface emissivity (equal to the surface long-wave absorptivity by the Kirchhoff law), F_{atm} is the view factor between the sky and the surface, I_{atm} is the radiation (W/m^2) emitted by the sky, F_{ground} is the view factor between the

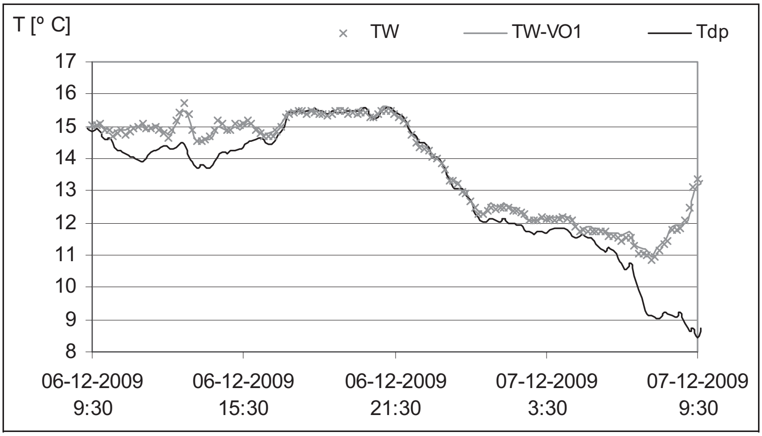

Figure 4. Temperature variation on the protected façade (*TW-VO1*) and unprotected façade (*TW*) and dew point temperature (*Tdp*), with cloudy sky, during one day of December 2009.

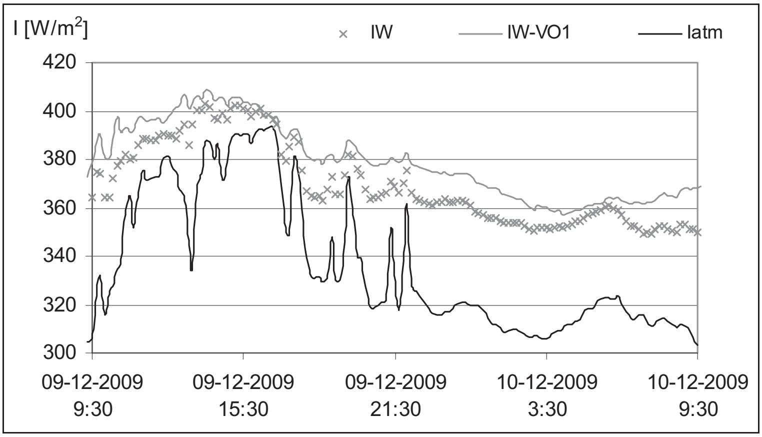

Figure 5. Long-wave radiation reaching the protected façade (*IW-VO1*) and unprotected façade (*IW*) and atmospheric radiation (I_{atm}), with clear sky, during one day of December 2009.

ground and the surface, I_{ground} is the radiation (W/m^2) emitted by the ground, F_O is the view factor between the obstacle and the surface, I_O is the radiation (W/m^2) emitted by the obstacle and I_b is the radiation (W/m^2) emitted by the building. The view factor between the *VO* and the surface depends on the obstacle dimensions and on its distance to the surface. It can be calculated considering two parallel surfaces with the same height and identical widths, using equation (3) adapted from Howell (1982). The radiation emitted by *VO* is ruled by the Stefan–Boltzmann law, considering the obstacle surface emissivity and temperature (equation (1)).

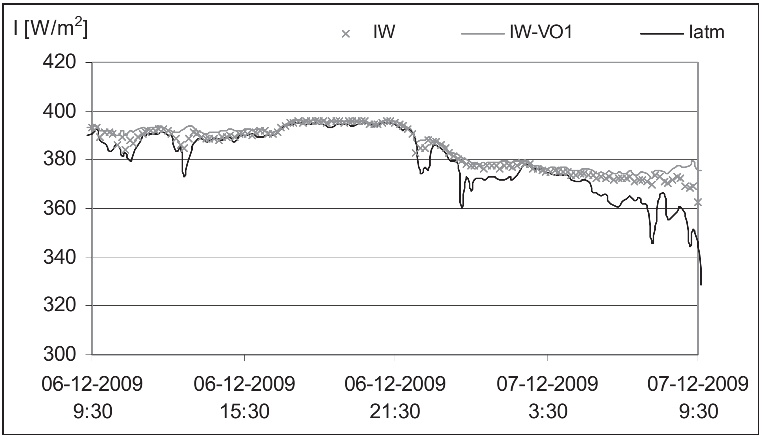

Figure 6. Long-wave radiation reaching the protected façade (*IW-VO1*) and unprotected façade (*IW*) and atmospheric radiation (*Iatm*), with cloudy sky, during one day of December 2009.

$$F_{VO} = \sqrt{1 + \left(\frac{h}{w}\right)^2} - \frac{h}{w} \tag{3}$$

where F_{VO} is the view factor between the VO and the surface, h is the distance (m) between the obstacle and the surface and w is the width (m) of the surfaces.

Exterior surface condensation can be analysed using psychrometry principles. When water vapour partial pressure of the air near the surface is greater than the water vapour saturation pressure at the surface, condensation will occur. According to Zheng et al. (2004), the difference between the water vapour partial pressure in the air and the water vapour saturation pressure on the surface may be called condensation potential, which implies condensation for positive values.

$$CP = P_v(air) - P_{sat}(surface) \tag{4}$$

where CP is the condensation potential (Pa), $P_v(air)$ is the water vapour partial pressure (Pa) in the air and $P_{sat}(surface)$ is the water vapour saturation pressure (Pa) on the surface.

The product of positive CP ($CP_{(>0)}$, Pa) by the corresponding interval of time ($\Delta t_{CP(>0)}$, h) may be called condensation potential equivalent (CPE, Pah). The accumulated value of positive CPE in time [$\Sigma(CPE > 0)$] allows estimating the amount of water vapour that is available to condensate in that period of time.

Figures 7 and 8 show the variation of positive CPE values in time, during two days of December 2009 (clear and cloudy sky). External condensation was more severe on the unprotected façade, as surface temperatures were lower. Figure 9(a) displays the accumulated positive CPE for the three test periods (May, August and

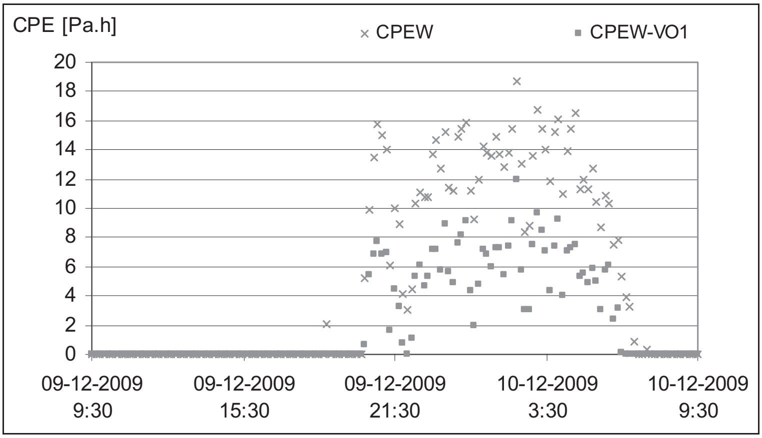

Figure 7. Positive *CPE* for the protected façade (*CPEW-VO1*) and unprotected façade (*CPEW*), with clear sky, during one day of December 2009.
CPE: condensation potential equivalent.

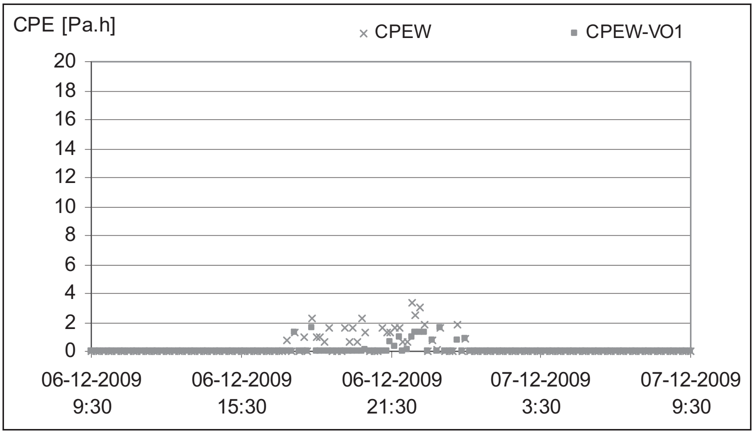

Figure 8. Positive *CPE* for the protected façade (*CPEW-VO1*) and unprotected façade (*CPEW*), with cloudy sky, during one day of December 2009.
CPE: condensation potential equivalent.

December 2009). It remarks the positive effect of the obstacle, by reducing condensation more than 50%.

With a distance of 2 m from the façade, the effect of the *VO2* was very similar. Figure 9(b) shows the accumulated positive *CPE* for the three test periods (June, July and December 2009). Here again, the obstacle had a positive effect on surface condensation as it was reduced. However, its influence was less obvious, as distance

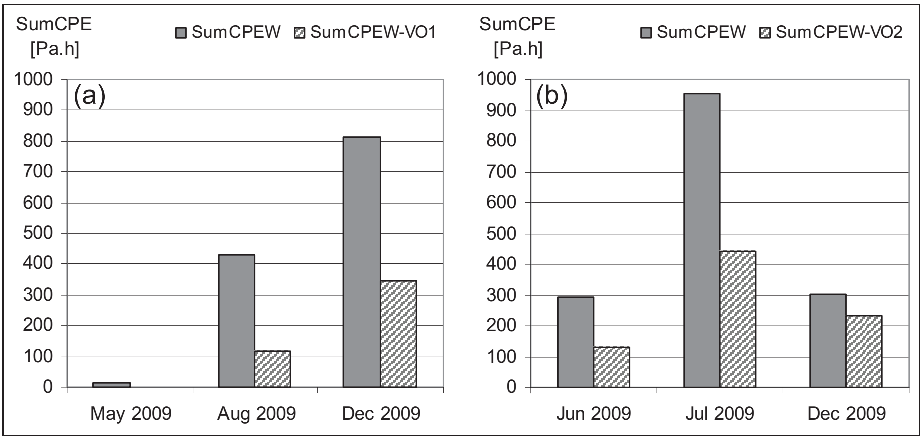

Figure 9. Sum of positive *CPE* for the unprotected façade (*SumCPEW*) and protected façade: (a) distance between the vertical obstacle and the façade equal to 1 m (*SumCPEW-VO1*) and (b) distance between the vertical obstacle and the façade equal to 2 m (*SumCPEW-VO2*).
CPE: condensation potential equivalent.

influences the view factor governing the radiation emitted by the obstacle that actually reaches the façade (equation (3)). Although the tests were not carried out simultaneously, equation (2) points to a stronger effect of *VO1* when restricting surface condensation. In the case under study, *VO1* had a view factor of 0.6 and *VO2* had a view factor of 0.4, which increases the amount of radiation that reaches the façade when protected by the closest obstacle and induces a surface temperature rise more obvious. During the test period of December, *VO2* had a small effect in reducing surface condensation (Figure 9(b)) as the sky was cloudy most of the time.

HOs. The surface temperature variation on the west façade, unprotected and protected by the plastic *HO*, is indicated in Figure 10, during one day of October 2009 with clear sky, and in Figure 11, during one day of October 2009 with cloudy sky. These graphs also indicate the dew point temperature (*Tdp*). As in the case of *VO*, also with *HO*, the unprotected façade always had lower surface temperature during the night. The extra source of long-wave radiation, emitted and reflected by the obstacle during the night, increased the temperature on the façade. When the sky was cloudy, the influence of the obstacle on the façade temperature was less intense.

During the day, the influence of the obstacle was different considering the season. During autumn and winter days, the *HO* did not change the surface temperature much, even increased it a few degrees, as solar radiation was absorbed and emitted towards the façade as long-wave radiation (Figure 10). During spring and summer days, the *HO* shaded the façade from solar radiation, decreasing surface temperature during the first hours of incident sun on the façade. Even so, the maximum temperature achieved was similar, due to absorbing/emitting and reflecting capacity of the

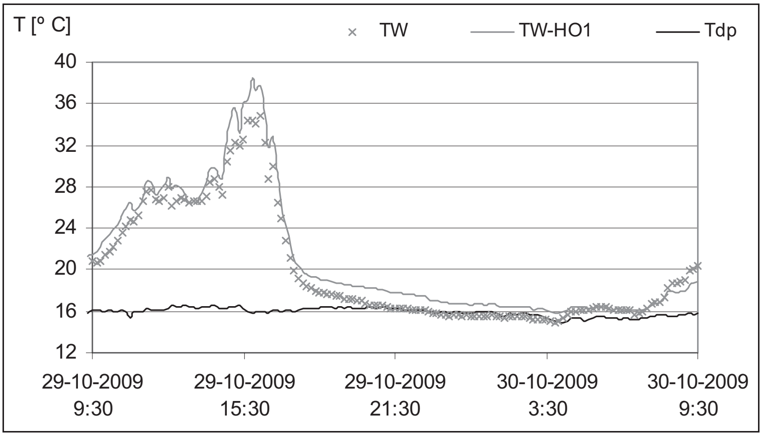

Figure 10. Temperature variation on the protected façade (*TW-HO1*) and unprotected façade (*TW*) and dew point temperature (*Tdp*), with clear sky, during one day of October 2009.

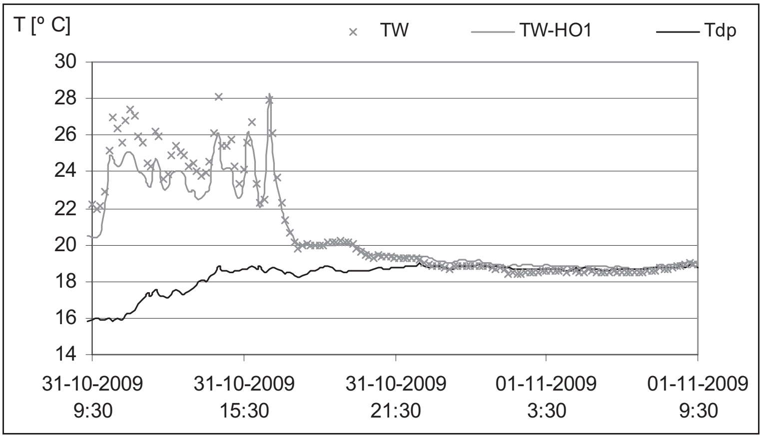

Figure 11. Temperature variation on the protected façade (*TW-HO1*) and unprotected façade (*TW*) and dew point temperature (*Tdp*), with cloudy sky, during one day of October 2009.

obstacle (Figure 12). It is important to say that these results were obtained using a thin element. Perhaps with a thicker one, the results might be different.

The role of the *HO* as an extra source of long-wave radiation is shown in Figure 13 that displays the long-wave radiation reaching the protected and unprotected façades. Higher amounts of radiation always reached the protected façade even when the sky was cloudy (Figure 14). Equation (2) rules the radiant balance on the façade protected by *HO* during the night, and the view factor is calculated by equation (5), adapted from Howell (1982), considering two

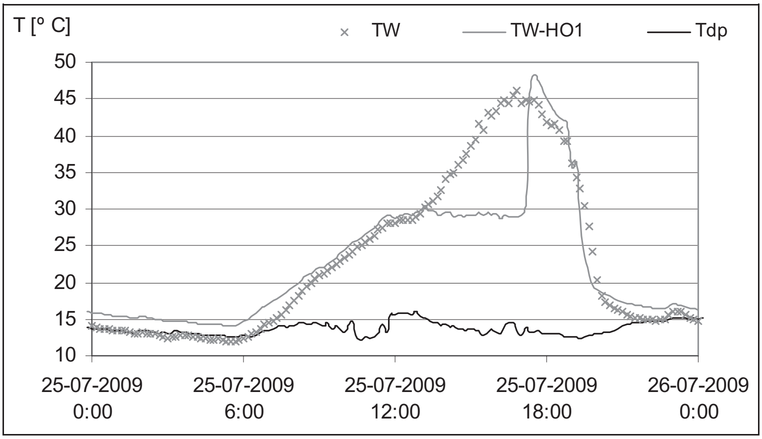

Figure 12. Temperature variation of the protected façade (*TW-HO1*) and unprotected façade (*TW*) and dew point temperature (*Tdp*), with clear sky, during one day of July 2009.

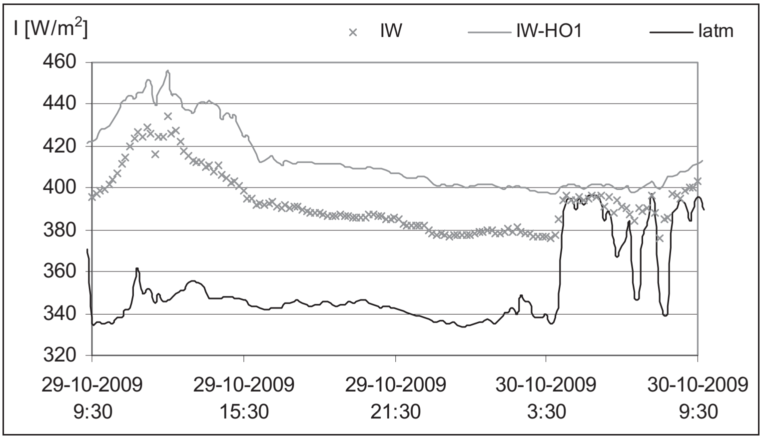

Figure 13. Long-wave radiation reaching the protected façade (*IW-HO1*) and unprotected façade (*IW*) and atmospheric radiation (I_{atm}), with clear sky, during one day of October 2009.

perpendicular surfaces. In the case under study, the view factor for the tested obstacle was 0.3. The radiation emitted by *HO* is given by the Stefan–Boltzmann law, considering the obstacle surface emissivity and temperature (equation (1)).

$$F_{HO} = \frac{1}{2} \times \left(1 + \frac{h}{w} - \sqrt{1 + \left(\frac{h}{w}\right)^2}\right) \tag{5}$$

where F_{HO} is the view factor between the *HO* and the surface, *h* is the obstacle depth (m) and *w* is the façade height (m).

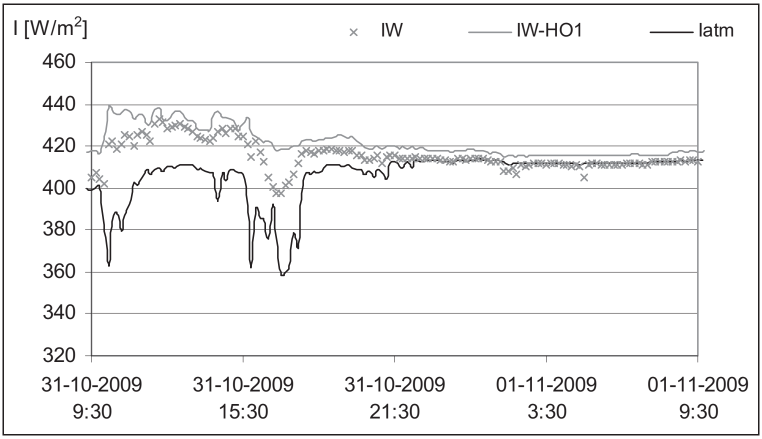

Figure 14. Long-wave radiation reaching the protected façade (*IW-HO1*) and unprotected façade (*IW*) and atmospheric radiation (I_{atm}), with cloudy sky, during one day of October 2009.

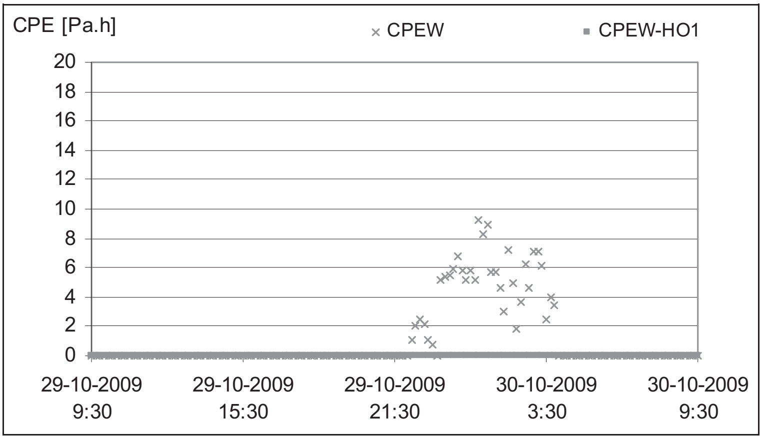

Figure 15. Positive *CPE* for the protected façade (*CPEW-HO1*) and unprotected façade (*CPEW*), with clear sky, during one day of October 2009.
CPE: condensation potential equivalent.

Figures 15 and 16 show the variation of positive *CPE* during two days of October 2009 (clear and cloudy sky). External condensation was more severe on the unprotected façade, as surface temperatures were lower. Figure 17(a) displays the accumulated positive *CPE* for the three test periods (April, July and October 2009). It remarks the positive effect of the obstacle, by reducing condensation almost 100%. For the metallic *HO*, the results were very similar. Figure 17(b)

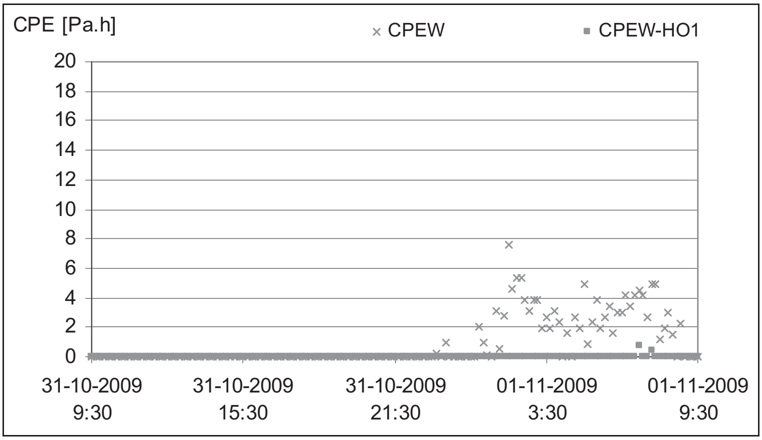

Figure 16. Positive *CPE* for the protected façade (*CPEW-HO1*) and unprotected façade (*CPEW*), with cloudy sky, during one day of October 2009.
CPE: condensation potential equivalent.

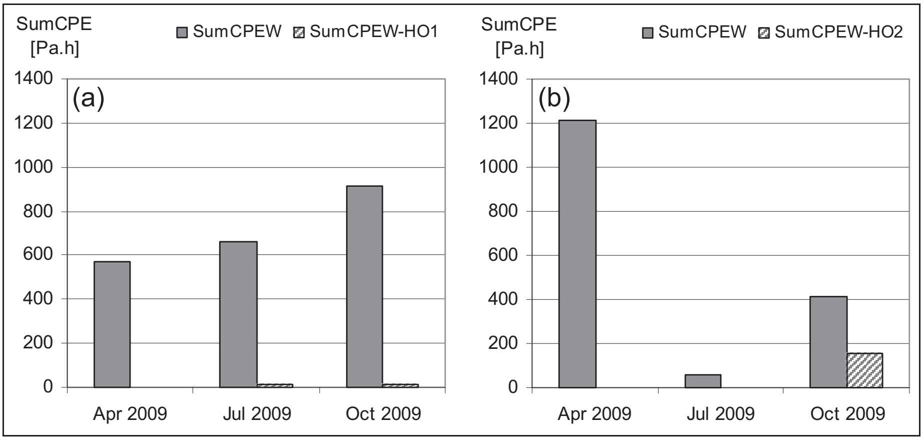

Figure 17. Sum of positive *CPE* for the unprotected façade (*SumCPEW*) and protected façade: (a) plastic horizontal obstacle (*SumCPEW-HO1*) and (b) metallic horizontal obstacle (*SumCPEW-HO2*).
CPE: condensation potential equivalent.

shows the accumulated positive *CPE* for the three test periods (April, July and October 2009). Here again, the obstacle had a positive effect on surface condensation as it was reduced.

It is not easy to evaluate if the influence of the metallic obstacle was more or less obvious than the effect of the plastic one, as tests were not performed simultaneously. Even so, it is possible to say by analysing equations (1) and (2) that as the plastic obstacle has higher emissivity than the metallic one, the radiation reaching the façade in the first case may be higher. Of course, if the effect of reflection ($\rho = 1 - \alpha$, for opaque surfaces) is considered, the differences between the effect of the two *HO* tested will be less important.

Results assessment

The results indicate that the effect of obstacles nearby a façade covered with ETICS reduces external surface condensation. The amount of long-wave radiation reaching the façade during the night is higher due to the emissive capacity of the obstacle. In fact, as the obstacle behaves like a grey body, it emits more radiation than the clear sky (see section 'Long-wave radiation exchange'). Even when there are clouds in the sky, the radiation reaching the façade is higher when there is a nearby obstacle as it works as an extra source of radiation. The higher amount of long-wave radiation incident in the surface increases its temperature and decreases the probability of dropping bellow dew point temperature. Therefore, external surface condensation is less intense.

The comparison between the effects of the four configurations tested (Table 1) is not very easy as the tests were not carried out simultaneously. However, the results showed that the different obstacle configurations influence surface condensation differently. Strictly analysing the radiant balance equation during the night (equation (2)), it is possible to compare the effect of the plastic obstacles (*VO1, VO2* and *HO1*). As *VO1* has the higher view factor and *HO1* the lower one, the first induces higher surface temperature on the façade, followed by *VO2* and finally by *HO1*. In reality, this interpretation may not be correct as the surfaces near *HO1* (Figure 2) also emit long-wave radiation and influence the balance at the surface. The results assessment also showed that longer distances from the façade decrease the positive effect of a *VO*. The emissivity of an obstacle surface may also have some influence on the phenomenon, as higher values imply more emission of long-wave radiation. Although no measurements were conducted in different locations of the building surface, farther from the obstacles, it can be assumed that the effect of the obstacle only has impact on surface temperatures when the obstacles are in the proximity of the façade and their dimensions are similar. Of course, the real influence of the obstacle is ruled by the view factor between the two surfaces, which considers their dimensions and the distance between them.

These results point that the existence of obstacles or other buildings near a façade may give raise to different amounts of condensation on its surface, which induces different rates of microorganisms' growth and may lead to stained patterns on the façade. This fact shall be considered by designers when applying ETICS on a building façade and the simulation of the phenomenon using software tools shall be possible. As there are no hygrothermal models available that allow simulating the effect of nearby obstacles in surface condensation on façades covered with ETICS, a new routine that can be used with any existing hygrothermal model was developed. The next paragraph presents the routine MOD.O that simulates the effect of nearby obstacles on exterior surface temperature and its validation by comparing the simulated and experimental results.

Numerical model to simulate the influence of nearby obstacles

Numerical model MOD.O

The routine MOD.O can be used with any existing hygrothermal model with the ability to simulate explicitly the radiative balance on the exterior surface. It calculates the increase in long-wave radiation due to the obstacle as a function of its geometry and emissivity of its surface. This extra amount of radiation is added to the atmospheric radiation that is an input of the hygrothermal models. In this routine, the explicit radiative balance on the surface, considering the presence of an obstacle, is simplified, and not all the radiation sources are taken into account. The effect of the cloudy sky, which increases the amount of radiation emitted by the sky and softens the obstacles' influence on surface temperature (see section 'Experimental study – assessing the influence of nearby obstacles'), is also included.

VOs. If the effect of the façade and of the ground is neglected, the radiation emitted by the VO that effectively reaches the façade can be calculated using equation (6), as a function of the view factor for opposed parallel surfaces (equation (3)) and the incident atmospheric radiation, considering the view factor between the sky and the surface (although equation (7) assumes a free unobstructed view of the quarter of a sphere from the façade to the sky, which do not occur when a VO with a comparable size to the building façade is near that façade, for the sake of simplicity this view factor is applied). It is assumed that all the radiation from the sky incident on the obstacle surface (back and front sides) is absorbed but only a portion, function of ε_{VO}, is emitted towards the wall.

$$I_{VO(inc)} = \varepsilon_{VO} \cdot (F_{atm} \cdot I_{atm}) \cdot F_{VO} \tag{6}$$

where $I_{VO(inc)}$ is the radiation (W/m^2) emitted by the VO that reaches the surface, ε_{VO} is the emissivity of the obstacle, F_{atm} is the view factor between the sky and the surface, I_{atm} is the radiation (W/m^2) emitted by the sky and F_{VO} is the view factor between the VO and the surface.

$$F_{atm} = \frac{1}{2} \cdot (1 + \cos\phi) \tag{7}$$

where F_{atm} is the view factor between the sky and the surface and ϕ is the inclination (°) of the surface.

Equation (8) allows calculating the increase in long-wave radiation due to a VO, which shall be added to the atmospheric radiation provided by the climatic data so the presence of the obstacle can be simulated. Considering the results obtained during the test campaign (section 'Experimental study – assessing the influence of nearby obstacles'), when the sky is cloudy, long-wave radiation that reaches the façade, with or without obstacle, is quite similar to atmospheric radiation. For that reason, during cloudy days, the increase calculated using equation (8) is no longer necessary. As cloud index is not always available in climatic data, equation (8) shall only be used when the difference between atmospheric radiation (hourly values from climatic data, I_{atm}) and long-wave radiation incident on the façade without obstacle (hourly values calculated by numerical simulation without MOD.O, $I_{inc(N/VO)}$) is above 1.5% of the annual average of the hourly atmospheric radiation from climatic data, $\overline{I_{atm}}$. An adjustment constant, a, was included in equation (8) to deal with the simplifications that were assumed. Its value, 1/3, was statistically determined to allow a good agreement between the measurements and the calculations.

$$\Delta I_{atm} = \varepsilon_{VO} \cdot (F_{atm} \cdot I_{atm}) \cdot F_{VO} \cdot a \quad \text{if } \left| I_{inc(N/VO)} - I_{atm} \right| > 1.5\% \cdot \overline{I_{atm}} \tag{8}$$

where ΔI_{atm} is the increase in long-wave radiation (W/m^2) due to the obstacle, $a = 1/3$ is an adjustment constant, $I_{inc(N/VO)}$ is the radiation (W/m^2) that reaches the surface if no obstacle is considered and $\overline{I_{atm}}$ is the annual average of the hourly atmospheric radiation (W/m^2) from climatic data.

HOs. For *HO*s, the effect of the ground is significant and must be considered to calculate the radiation emitted by the obstacle that effectively reaches the façade. The radiation emitted and reflected by the ground can be calculated as a function of atmospheric radiation (equation (9)).

$$I_{ground} = \varepsilon_{ground} \cdot \left(\varepsilon_{ground} \cdot I_{atm} \right) + \rho_{ground} \cdot I_{atm} \tag{9}$$

where I_{ground} is the radiation (W/m^2) emitted by the ground, ε_{ground} is the emissivity of the ground (equal to the ground long-wave absorptivity), I_{atm} is the radiation (W/m^2) emitted by the sky and ρ_{ground} is the long-wave reflectivity of the ground.

If the effect of the obstacle and of the façade is neglected and considering the emissivity of the ground close to the unit and the ground as an opaque surface ($\varepsilon_{ground} + \rho_{ground} = 1$), then the radiation emitted by the ground can be assumed as identical to the sky radiation ($I_{ground} \approx I_{atm}$).

The radiation emitted by the *HO* that effectively reaches the façade can be calculated using equation (10), as a function of the view factor for perpendicular surfaces (equation (5)), the incident atmospheric radiation and the emissivity of the obstacle. It is assumed that all the radiation emitted by the sky incident on the obstacle surface is absorbed but only a portion, function of ε_{HO}, is emitted towards the wall. Equation (11) allows calculating the increase in long-wave radiation due to the *HO*, which shall be added to the atmospheric radiation provided by the climatic data so the presence of the obstacle can be simulated. As in the case of *VO*s, also for *HO*s, an adjustment constant, a, was included in equation (11) to deal with the simplifications of the model. Its value was also statistically determined and is 1/3.

$$I_{HO(inc)} = \varepsilon_{HO} \cdot I_{atm} \cdot F_{HO} \tag{10}$$

$$\Delta I_{atm} = \varepsilon_{HO} \cdot I_{atm} \cdot F_{HO} \cdot a \quad \text{if } \left|I_{inc(N/HO)} - I_{atm}\right| > 1.5\% \cdot \overline{I_{atm}} \qquad (11)$$

where $I_{HO(inc)}$ is the radiation (W/m^2) emitted by the HO that reaches the surface, ε_{HO} is the emissivity of the obstacle, I_{atm} is the radiation (W/m^2) emitted by the sky (hourly values from climatic data), F_{HO} is the view factor between the HO and the surface, ΔI_{atm} is the increase in long-wave radiation (W/m^2) due to the obstacle, $a = 1/3$ is an adjustment constant, $I_{inc(N/HO)}$ is the radiation (W/m^2) that reaches the surface if no obstacle is considered (hourly values calculated by numerical simulation without MOD.O) and $\overline{I_{atm}}$ is the annual average of the hourly atmospheric radiation (W/m^2) from climatic data.

Table 2. Parameters used to calculate the increase in long-wave radiation due to obstacles.

Parameter	Value
ε_{VO}– plastic, brown	0.55[a]
ε_{VO}– rendering, light grey	0.85[a]
ε_{HO}– plastic, brown	0.55[a]
ε_{HO}– metallic	0.15[a]
F_{atm}	0.5
F_{VO} (distance from the façade = 1 m)	0.6
F_{VO} (distance from the façade = 2 m)	0.4
F_{VO} (distance from the façade = 18 m)	0.07
F_{HO}	0.3
a	1/3

[a]Values obtained by measuring the surface temperature, using a thermocouple and an infrared thermometer. The emissivity value was achieved by matching the temperature measured by the infrared thermometer to the one measured by the thermocouple (Barreira, 2010).

Validation of the model

Parameters for the simulation of the atmospheric radiation considering an obstacle. The numerical simulation of the surface temperature was performed using a commercial software. The effect of the obstacles was evaluated for the west façade of the building described in section 'Experimental study – assessing the influence of nearby obstacles', considering the real conditions of use. The atmospheric radiation inputted as climatic data was the sum of the real atmospheric radiation, measured by the LFC weather station (section 'Experimental study – assessing the influence of nearby obstacles'), and the increase in long-wave radiation due to the presence of the obstacles, calculated using model MOD.O (section 'Numerical model MOD.O') considering the parameters presented in Table 2. The increase in long-wave radiation used to assess surface temperature on the location W-HO (Figure 2) included the effect of the HO and the effect of the opposite façade that was considered as VO. As it is shown in Table 2, the effect of the opposite façade is

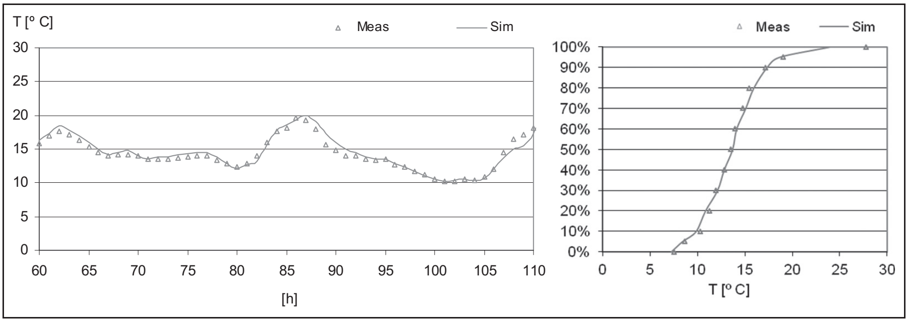

Figure 18. Variation in time and the cumulative distribution function of surface temperature on west façade with the *VO* at 1 m in December 2009 (measurements vs numerical simulation).

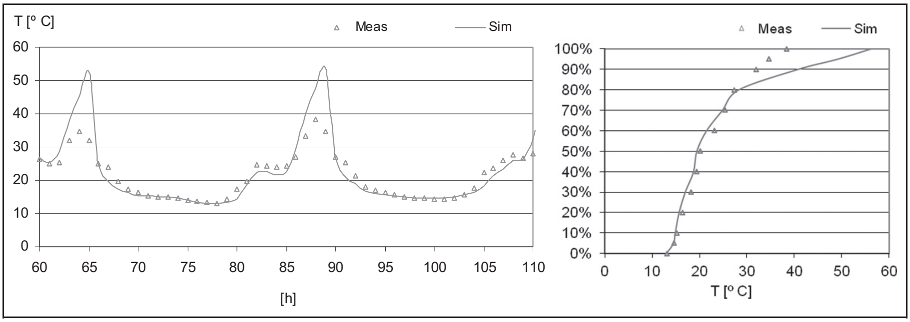

Figure 19. Variation in time and the cumulative distribution function of surface temperature on west façade with the *VO* at 1 m in August 2009 (measurements vs numerical simulation).

not very significant because the view factor is lower than the one obtained for the *HO*.

VOs. Figure 18 shows surface temperature variation, measured and calculated, on the west façade, protected by the *VO* at a distance of 1 m during two days of December 2009, and the cumulative distribution function. The results show that there is a good agreement between the simulated and the measured values, especially during the night when temperatures were lower. During daylight, the values are also very similar, mainly because the sky was cloudy most of the time and the sun's influence was less important. However, in August, the simulated values are considerably higher during daylight as the shade of the façade from solar radiation by the obstacle was not considered during the simulation (Figure 19). The measured and calculated values of the surface condensation (positive values of *CPE* as described in section '*VO*') are also very similar, with a deviation less than 10%

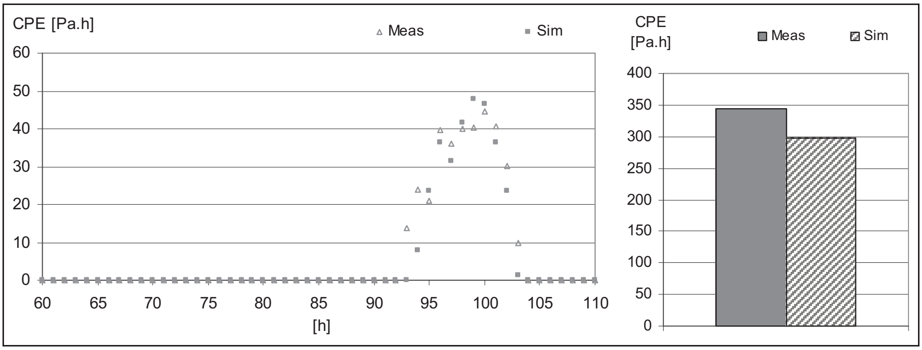

Figure 20. Variation in time and sum of positive *CPE* on west façade with the *VO* at 1 m in December 2009 (measurements vs numerical simulation).
CPE: condensation potential equivalent.

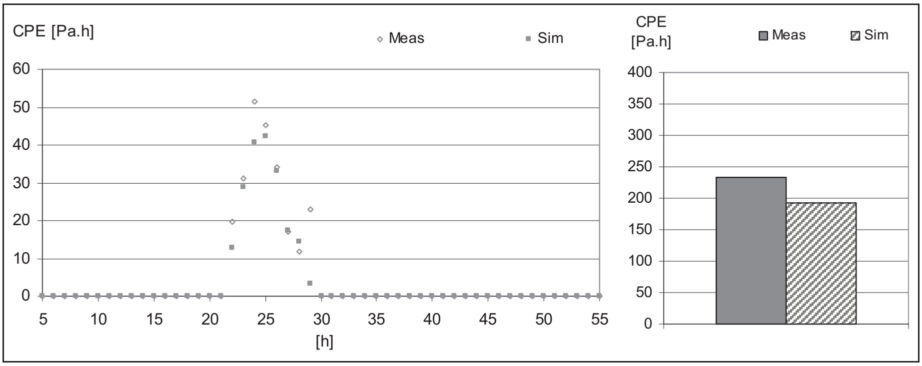

Figure 21. Variation in time and sum of positive *CPE* on west façade with the *VO* at 2 m in December 2009 (measurements vs numerical simulation).
CPE: condensation potential equivalent.

(Figure 20). The results obtained for the *VO* at a distance of 2 m are similar to the ones for a distance of 1 m, as shown in Figure 21.

HOs. Figure 22 shows surface temperature variation, measured and calculated, on the west façade, shaded by the plastic *HO*, during two days of October 2009 and the cumulative distribution function. As for *VO*s, also for HOs, the results show that there is a good agreement between the simulated and the measured values, especially during the night. During warmer months, the simulated values are also considerably higher during daylight as the shade of the façade from solar radiation by the obstacle was not considered during the simulation (Figure 23). The measured and calculated values of the surface condensation are also very similar

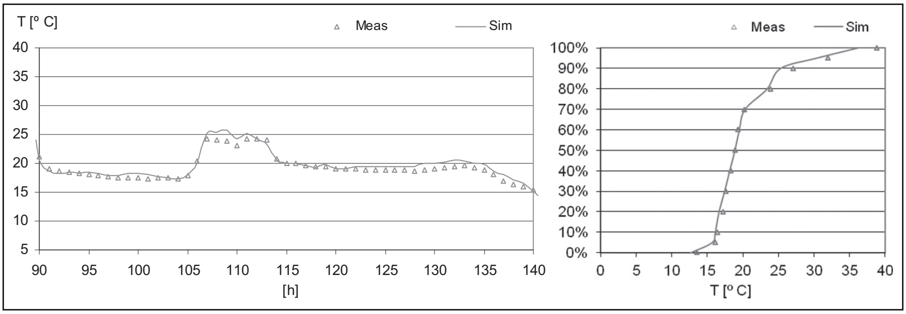

Figure 22. Variation in time and the cumulative distribution function of surface temperature on west façade with the plastic *HO* in October 2009 (measurements vs numerical simulation).

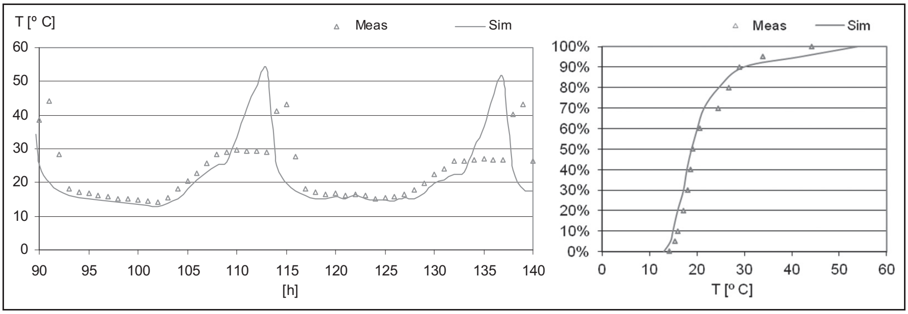

Figure 23. Variation in time and the cumulative distribution function of surface temperature on west façade with the plastic *HO* in July 2009 (measurements vs numerical simulation).

(Figure 24). The results obtained for the metallic *HO* are also quite similar, as shown in Figure 25.

Practical application of MOD.O

The practical use of MOD.O was assessed by applying it to three real buildings located in the University of Porto campus. The buildings are covered with ETICS, and their north façade is faced with other buildings of the campus with different dimensions (Figure 26 and Table 3). The simulations were performed considering the climatic data provided by the LFC weather station during 2010. To calculate the increase in long-wave radiation due to the *VO*s, equation (8) was used, considering the parameters displayed in Table 3, the emissivity of the obstacles of 0.85 (façades covered with ETICS are painted with very light grey; the value was measured using a thermocouple and an infrared thermometer as described in Barreira, 2010), the view factor between the sky and the surface of 0.5 and the correction constant, *a*, of 1/3.

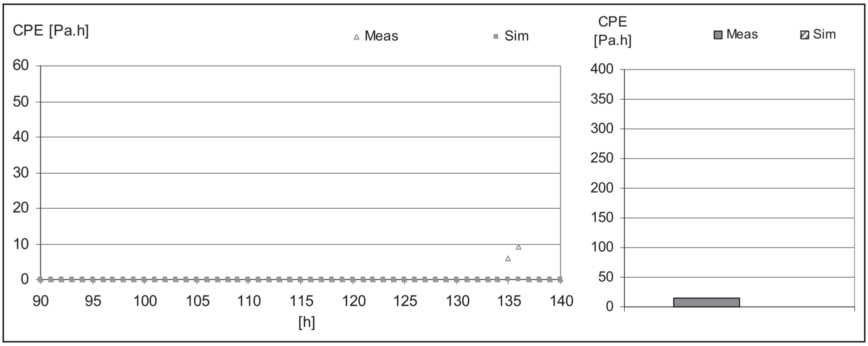

Figure 24. Variation in time and sum of positive *CPE* on west façade with the plastic *HO* in October 2009 (measurements vs numerical simulation).
CPE: condensation potential equivalent.

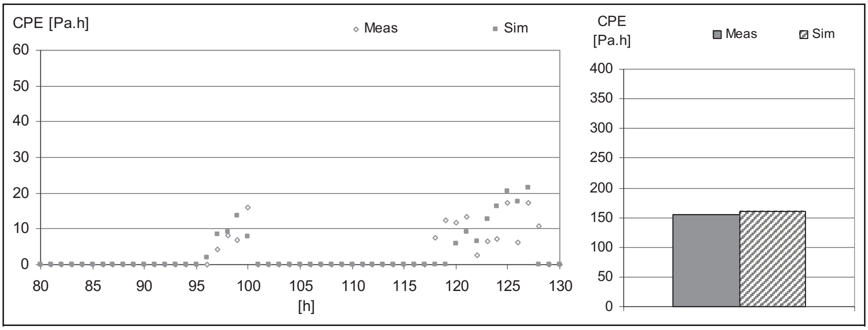

Figure 25. Variation in time and sum of positive *CPE* on west façade with the metallic *HO* in October 2009 (measurements vs numerical simulation).
CPE: condensation potential equivalent.

$$F_{ij} = \frac{1}{A_i} \cdot \int_{A_i} \int_{A_j} \frac{\cos\theta_i \cdot \cos\theta_j}{\pi^2 \cdot S} dA_j dA_i \tag{12}$$

where F_{ij} is the view factor, A_i and A_j are the areas (m^2), θ_i and θ_j are the angles (rad) and S is the distance (m), according to the formulation available in Howell (1982) to calculate the view factor between two finite areas in arbitrary configuration.

Figure 27 shows the monthly accumulated positive values of *CPE* on the north façade of Buildings B1, B2 and B3 (Figure 26) during 2010, obtained by numerical simulation using the model MOD.O in connection with a commercial hygrothermal simulation tool. External surface condensation is much more intense on B1, which does not have any building in the opposite side, and almost insignificant on

Table 3. Description of the buildings under study and parameters for the numerical simulation

Building	Obstacle	View factor – F_{VO}
B1	None	–
B2	Shorter building	0.38 (equation (12))
B3	Building with the same size	0.59 (equation (3))

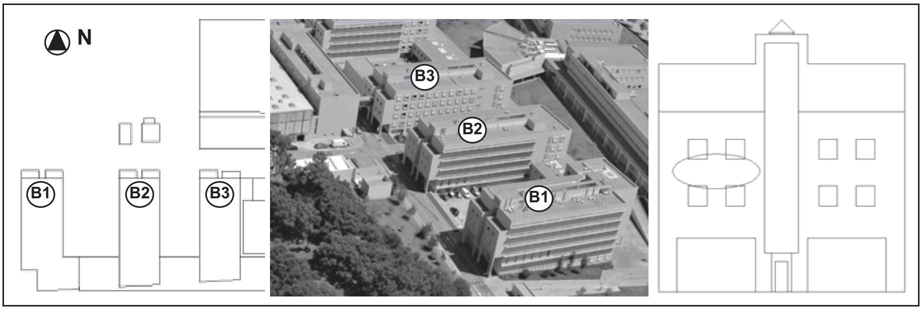

Figure 26. Location of the buildings under study and area on each façade that was photographed.

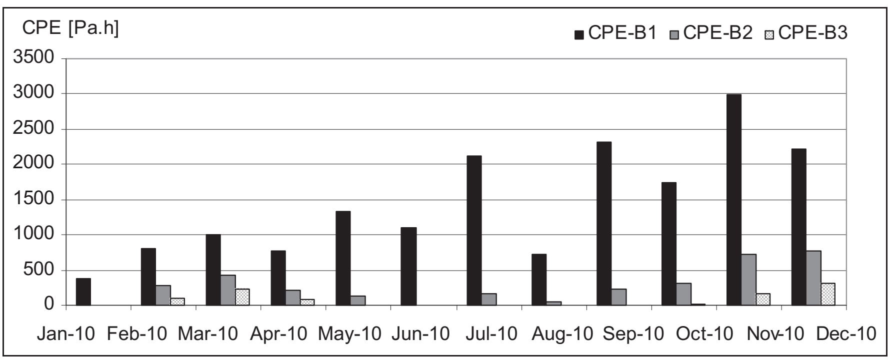

Figure 27. Monthly accumulated positive values of *CPE* on the north façade of Buildings B1, B2 and B3 during 2010 (numerical simulation results).
CPE: condensation potential equivalent.

B3, which has a similar building facing the surface under study. Condensation on B2 is in between the other two as the obstacle is a building smaller than the one under study.

These results are compatible with the degree of defacement due to biological growth on the north façade of the three buildings under study. Photographs of

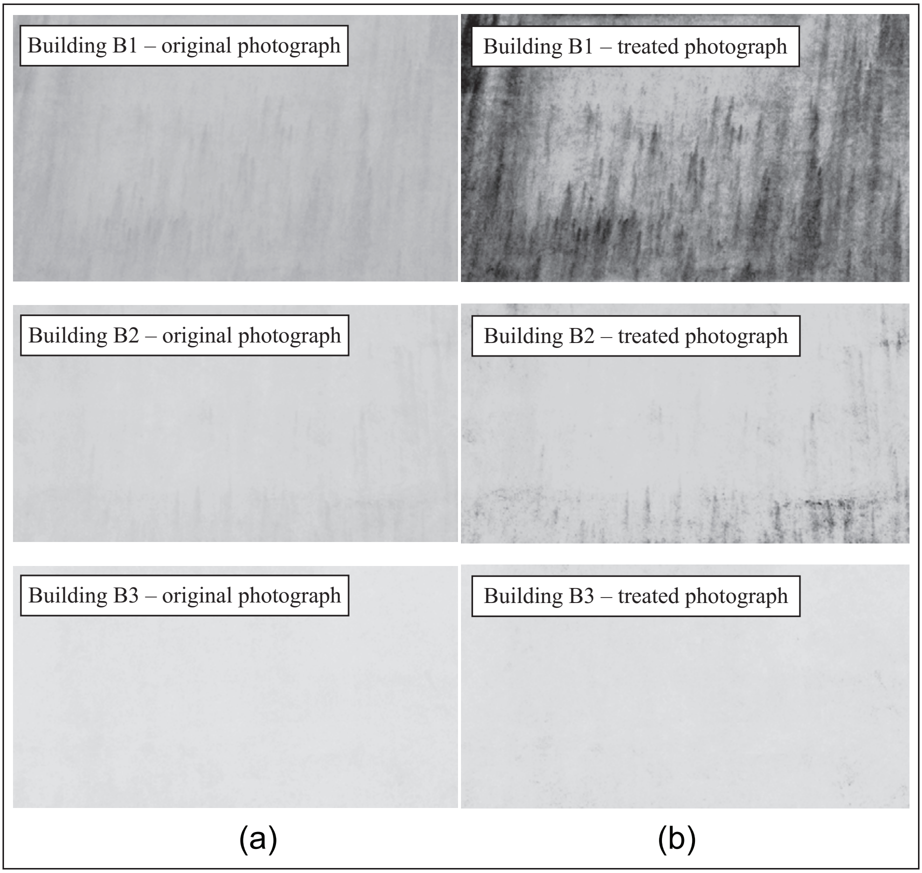

Figure 28. Defacement of the north façade of the three buildings under study (B1, B2 and B3): (a) original photographs and (b) photographs after being treated with an image software tool.

similar areas on the three façades were taken (Figure 26), at the same day and hour. Figure 28 shows these photographs before and after being treated with an image software tool to highlight the defacement of the surface. The images show that the façade of B1 is significantly more defaced than the other two. The differences between B2 and B3 are less important although B3 has slightly less biological colonisation.

Conclusion

ETICS is applied regularly in Portuguese buildings. However, despite their advantages, the cladding defacement due to biological growth is a very severe pathology. The development of microorganisms on ETICS depends on its surface moisture for a certain period of time, which is influenced by vapour condensation, wind-driven rain, drying process and rendering properties.

This article describes the results of a test field campaign to assess the influence of obstacles near a façade on surface condensation. They showed that obstacles restrict the condensation as they are a source of long-wave radiation. Higher amount of radiation incident on the surface increases the absorbed part and reduces the negative radiant balance on the façade, which leads to a smaller drop in the surface temperature and consequently decreases condensation. The results also showed that different obstacle configurations have different effects on surface condensation, and therefore, the existence of obstacles or other buildings near a façade may give raise to different amounts of condensation on its surface, which induces different rates of microorganisms' growth. This may lead to stained patterns on the façade.

A physical model to simulate the influence of nearby obstacles on a façade covered with ETICS, MOD.O, was developed to help designers who intend to apply this technology. This new routine can be used with any existing hygrothermal model with the ability to simulate explicitly the radiative balance on the exterior surface. It allows calculating the increase in long-wave radiation due to the obstacle, as a function of its geometry and emissivity of its surface, which shall be added to the atmospheric radiation that is an input of the hygrothermal models. The results of the numerical simulation performed using the atmospheric radiation calculated by MOD.O are very similar to the ones obtained in the 'in situ' test campaign. Values of surface temperature and surface external condensation, using *CPE* concept, were compared for different obstacle configurations: *VO* at 1 and 2 m from the building surface and *HO* with two different emissivities. There is a good agreement between the measured and calculated values of the surface temperature and external surface condensation. Only during daylight, when the sky is clear, the values of measured and calculated surface temperature differ considerably as the model does not considers the shading of the façade by the obstacle.

Using MOD.O applied to a real case study in University of Porto campus, it was possible to assess the defacement of different façades shaded by buildings with different configurations. The results of the numerical simulation performed for three buildings pointed different degrees of surface condensation, which is in accordance with biological colonisation on the façades that is visually detected. These results point that MOD.O is a valid tool to be used by designers to predict the behaviour of a façade covered with ETICS shaded by obstacles.

Although good results are obtained using MOD.O to simulate the effect of the obstacles on exterior surface temperature of a façade covered with ETICS, the limitations of this study impose that more work must be done to the full validation of the model. In the future, new obstacle configurations must be tested, namely, the effect of smaller or bigger obstacles located farther or nearer the façade. It is also necessary to assess the importance of the obstacle's influence on the regions of the building surface that are farther from the obstacle. Real case studies, with thicker obstacles, must also be evaluated to guarantee that in real conditions of use, the effect of obstacles is also significant.

Funding

This study received the financial support from Fundação para a Ciência e Tecnologia (FCT) through the doctoral grant SFRH/BD/39904/2007.

References

Barberousse H, Ruota B, Yéprémianb C, et al. (2007) An assessment of façade coatings against colonisation by aerial algae and cyanobacteria. *Building and Environment* 42: 2555–2561.

Barreira E (2010) *Biological defacement of façades covered with external thermal insulation systems due to hygrothermal behaviour*. PhD Thesis, University of Porto – Faculty of Engineering, Portugal (in Portuguese).

Barreira E, Delgado JMPQ and Ramos NMM (2012) Exterior condensations on façades: numerical simulation of the undercooling phenomenon. *Journal of Building Performance Simulation*. Epub ahead of print 26 May 2011. DOI: 10.1080/19401493.2011.560685.

Barreira E and Freitas VP (2013) Experimental study of the hygrothermal behaviour of External Thermal Insulation Composite Systems (ETICS). *Building and Environment*. Epub ahead of print 9 February 2013. Available at: http://dx.doi.org/10.1016/j.buildenv.2013.02.001

Becker R (2003) Patterned staining of rendered facades: hygro-thermal analysis as a means for diagnosis. *Journal of Building Physics* 26(4): 321–341.

Blaich J (1999) *La détérioration des bâtiments – Analyse et prevention*. Dubendorf, Suisse: EMPA.

Freitas VP (2002) *Isolamento Térmico de Fachadas pelo Exterior – Reboco Delgado Armado Sobre Poliestireno Expandido (ETICS)*. Relatório HT 191A/02, December 2002. Porto: Prof. Eng° Vasco Peixoto de Freitas, Lda.

Hagentoft C-E (2001) *Introduction to Building Physics*. Lund, Sweden: Studentlitteratur.

Hens H and Carmeliet J (2002) Performance prediction for masonry walls with EIFS using calculation procedures and laboratory testing. *Journal of Building Physics* 25(3): 167–187.

Holm A, Zillig W and Kunzel H (2004) Exterior surface temperature and humidity of walls – comparison of experiment and numerical simulation. In: *Proceedings of performance of exterior envelopes of whole buildings IX, ASHRAE*, Clearwater, FL, 5–10 December 2004.

Howell J (1982) *A Catalog of Radiation Heat Transfer Configuration Factors*. Austin, TX: The University of Texas at Austin. Available at: http://www.me.utexas.edu/~howell/index.html (accessed 25 January 2010).

Krus M, Rosler D and Sedlbauer K (2006) New model for the hygrothermal calculation of condensate on the external building surface. In: *Proceedings of third international building physics conference – research in building physics and building engineering*, Concordia University, Montreal, Canada, 27–31 August. London, UK: Taylor & Francis Group, pp. 329–333.

Kunzel H and Sedlbauer K (2001) Biological growth on stucco. In: *Proceedings of performance of exterior envelopes of whole buildings VIII: integration of building envelopes, ASHRAE*, Clearwater, FL, 2–7 December 2001.

Kunzel H, Schmidt Th and Holm A (2002) Exterior surface temperature of different wall constructions – comparison of numerical simulation and experiment. In: *Proceedings of 11th symposium of building physics*, Technische Universitat Dresden, Dresden, Germany, 26–30 September 2002, vol. 1. Dresden, Germany: Eigenverlag der TU Dresden, pp. 441–449.

Sedlbauer K and Krus M (2002) Mold growth on ETICS (EIFS) as a result of 'bad workmanship'? *Journal of Building Physics* 26(2): 117–121.

Venzmer H, von Werder J, Lesnych N, et al. (2008) Algal defacement of façade materials – results of long term natural weathering tests obtained by new diagnostic tools. In: *Proceedings of 8th symposium on building physics in the Nordic countries*, Danmarks Tekniske Universitet, Copenhagen, Denmark, 16–18 June 2008, vol. 1. DTU Byg Report R-189, Lyngby, Denmark, pp. 277–284.

Zheng R, Janssens A, Carmeliet J, et al. (2004) An evaluation of highly insulated cold zinc roofs in a moderate humid region – part I: hygrothermal performance. *Construction and Building Materials* 18(1): 49–59.

Zillig W, Lenz K and Krus M (2003) Condensation on façades – influence of construction type and orientation. In: *Proceedings of the 2nd international conference on building physics – Research in building physics,* 14–18 September 2003, Antwerp, Belgium. The Netherlands: AA Balkema, pp. 437–444.